

Article

# Powder XRD Structural Study of Ba<sup>2+</sup> Modified Clinoptilolite at Different Stages of the Ion Exchange Process Conducted at Two Temperature Regimes—Room Temperature and 90 °C

Louiza Dimowa <sup>1,\*</sup>, Yana Tzvetanova <sup>1</sup> , Ognyan Petrov <sup>1</sup>, Iskra Piroeva <sup>2</sup> and Filip Ublekov <sup>3</sup>

<sup>1</sup> Institute of Mineralogy and Crystallography, Bulgarian Academy of Sciences, 1113 Sofia, Bulgaria; yana.tzvet@gmail.com (Y.T.); opetrov@dir.bg (O.P.)

<sup>2</sup> Academician Rostislav Kaishev Institute of Physical Chemistry, Bulgarian Academy of Sciences, 1113 Sofia, Bulgaria; ipiroeva@ipc.bas.bg

<sup>3</sup> Institute of Polymers, Bulgarian Academy of Sciences, 1113 Sofia, Bulgaria; fublekov@polymer.bas.bg

\* Correspondence: louiza.dimova@gmail.com

Received: 30 September 2020; Accepted: 20 October 2020; Published: 22 October 2020



**Abstract:** Partial and almost complete barium exchange on clinoptilolite is performed and structurally studied for different durations (2 h, 24 h, 72 h, 168 h, 12 d, 22 d) at room temperature and 90 °C of the ion exchange process. Continuing ion exchange up to the 22nd day is proved by EDS analyses data and powder XRD (intensity changes of 020 and 200 peaks). Rietveld structure refinement was first performed on the maximum Ba exchanged clinoptilolite at 90 °C for 22 days (3.04 atoms per unit cell). Four barium positions and 9 H<sub>2</sub>O sites were refined. The split positions Ba<sub>2</sub> and Ba<sub>K</sub> (around M3 site in channel C) were found mostly occupied by 2.23 atoms per unit cell. The rest of refined samples showed different occupations of the positions of incoming Ba<sup>2+</sup> and outgoing cations (Na<sup>+</sup>, Ca<sup>2+</sup>, K<sup>+</sup>, Mg<sup>2+</sup>) during ion exchange, describing extra-framework cationic movements, which are released easily without preferable directions. The exchanges at 90 °C and room temperature were found proceeding similarly up to the 2nd hour, but then at room temperature the process is slowed and at 22nd day 1.64 barium atoms per unit cell are structurally refined.

**Keywords:** clinoptilolite; Ba-exchange; powder XRD; Rietveld; crystal structure

## 1. Introduction

Natural zeolites are one of the most interesting mineral groups in the mineralogical classifications with more than 70 species. Some of them like clinoptilolite, mordenite, and chabazite form huge deposits in many countries including Bulgaria, which are of economic value and are a challenge for scientific investigations. Clinoptilolite forms about 90% of the world deposits of natural zeolite material used in different utilization procedures.

The specific microporous structure of these minerals is characterized by SiO<sub>4</sub><sup>4-</sup> and AlO<sub>4</sub><sup>5-</sup> tetrahedra forming framework with channels and cages in which cations compensating the framework charge are occupying specific sites and are coordinated by H<sub>2</sub>O molecules.

This structural configuration is a prerequisite of unique properties of natural zeolites—ion exchange, sorption, adsorption, catalytic activity, surface modification, reversible dehydration-rehydration, etc. [1–5].

The crystal structure of clinoptilolite was first determined by Alberti [6] using single crystal XRD analysis. The author proved that clinoptilolite is isostructural with heulandite displaying HEU-type structure according to the recent structural classification of natural zeolites. Three cationic positions

were proved in the channels with one of them new, compared to heulandite. A little later Koyama and Tacheuchi [7] performed a new structural analysis of clinoptilolite crystals proving the same structure but finding a fourth cationic position, which they attributed to magnesium occupation. Using powder XRD data, Petrov et al. [8] refined the structure of sedimentary microcrystalline clinoptilolite and also proved the monoclinic structure (space group C2/m) as the previous authors and found increased  $Mg^{2+}$  content in position M4 proposed by Koyama and Tacheuchi [7].

Over the years, there have been many research papers published reporting results for ion-exchange of clinoptilolite with large spectrum of cations (alkaline, alkaline-earth, metals, etc.). However, studies on ion-exchange with large bivalent cations like  $Ba^{2+}$  (ionic radius 1.35 Å) are rare [9,10]. Hawkins and Ordonez [11] first prepared Ba-exchanged clinoptilolite and observed substantial decrease in the intensity of 020 diffraction line. Later, Petrov et al. [12] refined the structure of Ba-exchanged sedimentary clinoptilolite using powder XRD data and proved the distribution of barium ions in the plane of symmetry of the structure at around the potassium position (site M3 according to Koyama and Tackeuchi [7]) replacing the  $K^+$  ions.

Cerri et al. [13] performed an interesting study on solid-state transformation of (NH<sub>4</sub>, Ba)-clinoptilolite upon heat treatment. The authors found increased thermal stability of Ba-dominated clinoptilolite—the higher the barium content, the higher the amorphization temperature.

Naturally occurring Ba-clinoptilolite has still not been found or proved. However, Barium containing clinoptilolite with Ba contents up to 1.83 wt% BaO (0.33  $Ba^{2+}$  per unit cell) was discussed [14] on a series of samples in Miocene sediments from the Yamato Basin of the Japan Sea—ODP Site 797. Similar content (0.44  $Ba^{2+}$  per unit cell) was reported for clinoptilolite sample from Beli plast deposit, Bulgaria [15].

However, for the heulandite, the isostructural counterpart of clinoptilolite, it was proved to have natural representative discussed by Larsen et al. [16]. The authors described this find in detail including single crystal XRD refinement of the Heulandite-Ba new zeolite species in the heulandite series, occurring as an accessory mineral in hydrothermal veins of the Kongsberg silver deposit, Buskerud County, Norway. They found that Heulandite-Ba is monoclinic, C2/m. Their sample is almost with the same Ba concentration (2.20 Ba per unit cell) with the Ba-exchanged clinoptilolite (2.54 Ba per unit cell) of Petrov et al. [12]. In both samples all Ba is accumulated in the centre of the C ring distributed among three cation sites.

In order to find additional structural specificity of distribution of barium ions in clinoptilolite structure during different regimes of ion-exchange, namely temperature and duration, we specify the purpose of the present paper to study Bulgarian microcrystalline clinoptilolite from Beli Plast deposit during barium exchange processes applying Rietveld powder XRD structural control. The results may shed light on specific site occupation of  $Ba^{2+}$  ions, probably governed by its large ionic radius rather than its bivalence character. This data may answer also to the found higher thermal stability of Ba-clinoptilolite.

The changes in the occupancy of the cationic positions during the ion exchange process can contribute to the elucidation of the logistic and transport possibilities of barium and outgoing cations in the structure of clinoptilolite at room temperature (RT) and 90 °C. The successive changes in the populations of the cationic positions during the ion exchange process are connected with the movement of the cations in clinoptilolite structure. This is studied by the methods of X-ray diffraction analysis.

We apply specific interpretation of Ba-clinoptilolite based on the gallery model proposed by Kirov et al. [17]. The authors show that the HEU structural type as well as the structures of other pseudo-layered zeolites, differ substantially from both the channel type structures (MOR, LTL, MAZ, LAU, etc.) and the cage type ones (CHA, FAU, LTA, etc.). The channel model of the porous space applied to HEU-type zeolites gives a topologically imprecise idea of the architecture of the porous space and misleads in the evaluation of its “logistical” capabilities—movement and positioning of exchangeable cation [17]. Consideration of the partially exchanged barium structures in our study up

to the almost completely exchanged one is presented associated with the intracrystalline diffusion of cations. Understanding this process can be facilitated by adopting the gallery space model.

At last, the aim of this study is to obtain new structural and crystal chemical data about the positioning of exchangeable large bivalent cation like  $\text{Ba}^{2+}$ , which may help for structural characterization of naturally occurring Ba-clinoptilolite if found analogous to the already proved natural Ba-heulandite.

## 2. Materials and Methods

### 2.1. Materials

The studied material is clinoptilolite tuff from Beli Plast deposit (Eastern Rhodopes, Bulgaria) rich in clinoptilolite (80 wt%, proved by quantitative XRD analysis). After grinding and sieving, the fraction with grain size 0.032–0.016 mm (richest in clinoptilolite) was used for further experiments. Additional mineral phases present in the selected fraction were removed by heavy liquid separation giving only clinoptilolite and small amount (6–7 wt%) of opal-C. The last stage was the removal of opal-C using chemical treatment with solution of NaOH. All the above stages were described in detail by Dimowa et al. [18].

### 2.2. Cation Exchange

The cation exchange experiments were performed with 8 g of clinoptilolite using 240 mL 0.5 M solution of  $\text{BaNO}_3$  for temperature regimes—room temperature (RT) and 90 °C. The solution was freshened at 48 h, 96 h, and 192 h. Samples for analyses were taken at 2 h, 24 h, 72 h, 168 h, 12 days, and finally at the 22nd day. Each separated sample was carefully washed with hot distilled water.

### 2.3. SEM/EDS

Chemical analysis of each Ba exchanged clinoptilolite sample was done with JEOL JSM6390 (JEOL technics Ltd., Tokyo, Japan) scanning electron microscope (SEM) coupled with an Oxford Instruments (Oxford Instruments Analytical Limited, High Wycombe, Buckinghamshire, UK) energy-dispersive X-ray (EDX) analyzer, with an acceleration voltage of 20 kV.

### 2.4. X-ray Diffraction Studies

Powder XRD investigations were performed using Bruker D8 Advance ECO (Bruker AXS GmbH, Karlsruhe, Germany) scanning diffractometer, operating at 40 kV and 25 mA in Bragg–Brentano geometry with Ni-filtered  $\text{Cu K}\alpha$  radiation and a LynxEye-XE (Bruker AXS GmbH, Karlsruhe, Germany) scanning detector over the  $2\theta$  range of 8–100° with a scanning rate of 0.01°/1 s.

Structural refinements of unit-cell parameters, atomic positions, and site occupancies of cations and  $\text{H}_2\text{O}$  molecules in clinoptilolite structure at different stages of barium exchange were performed using Rietveld based [19,20] refinement with Topas software (version 4.2). [21]. The background was fitted by a Chebyshev polynomial with 20 coefficients and the pseudo-Voigt peak function was applied. For all Ba-exchanged clinoptilolite samples, the refinement started with the model for Ba-heulandite of Larsen et al. [16] (ICSD #152331) and for the original Na, Mg positions and some  $\text{H}_2\text{O}$  molecules the clinoptilolite structural model of Koyama and Takeuchi [7] (ICSD #100096) was used.

## 3. Results

### 3.1. Powder XRD and EDS Data of Ba Exchanged Clinoptilolite

The clinoptilolite sample subjected to ion exchange with barium cations for a period up to the 22 days (at RT and 90 °C) undergoes exchange, which proceeds all the time with different speed confirmed from both the EDS analyses and the marked intensity changes of some peaks in the powder XRD patterns of samples selected at different exchange times (Figure 1). On Figure 1 the peaks 020 and 220

are indicated, which are most influenced by the degree of barium exchange. Comparing the patterns of the material from 2 h of exchange and the next taken at 24 h, 72 h, 168 h, 12 days, and 22 days, we notice significant intensity changes in the above peaks in the diffraction patterns—020 decreases while 220 increases (Table 1).

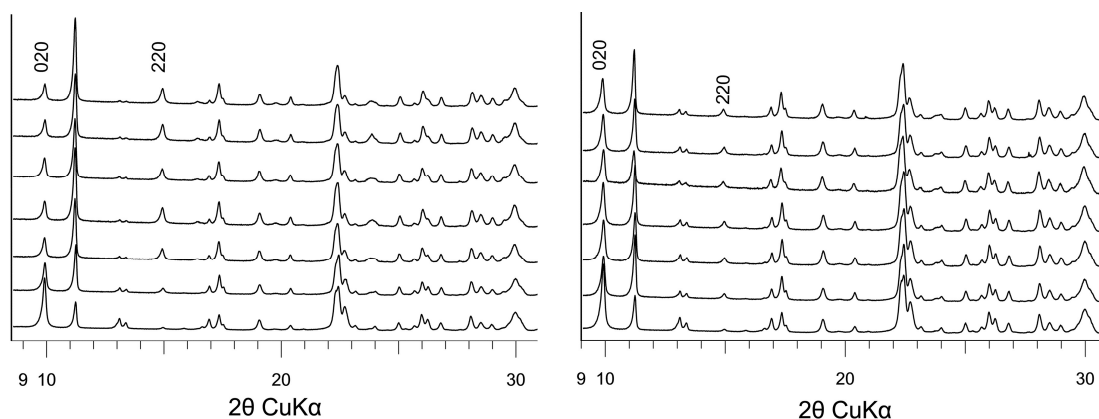


**Figure 1.** Powder XRD patterns of the purified clinoptilolite (bottom) and the Ba-exchange sequence of clinoptilolite at 90 °C (**left**) and room temperature (RT) (**right**) (from second pattern to top—2 h, 24 h, 72 h, 168 h, 12 days, and 22 days, of exchange).

**Table 1.** Integral Intensities of 020 and 220 peaks of Ba-clinoptilolite for different exchange times and temperatures.

Ion Exchange Duration (h)/Temperature (°C)	Integral Intensities	
	020	220
initial	125.54	13.26
2 90	84.97	25.07
2 RT	93.82	22.53
24 90	66.1	42.51
72 90	63.11	48.76
168 90	61.17	52.36
288 90	57.21	53.04
528 90	56.89	58.55
528 RT	82.22	28.7

Selected powder XRD patterns of Ba-clinoptilolite at different exchange regimes are shown on Figure 2. The sample exchanged at 90 °C for 24 h displays lowest intensity of 020 peak compared to the other two Ba-exchanged samples. The sample at 90 °C for 2 h and at RT for 22 days show almost equal intensity of this peak. Exact intensity values of 020 and 220 calculated by profile fitting [22] and normalized to the intensity of the complex peak at  $2\theta = 22.39$  ( $d = 3.97$  Å) are given in Table 1.

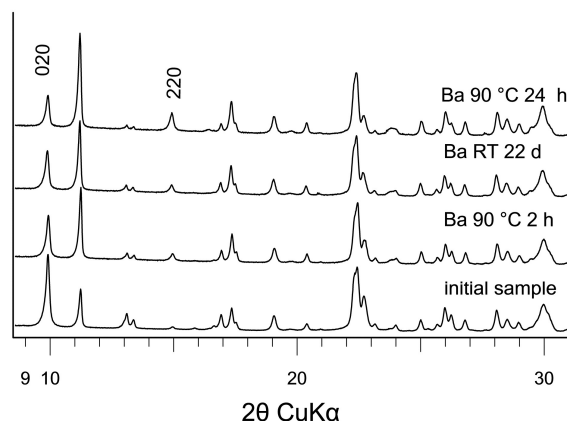


Figure 2. Selected powder XRD patterns of Ba-exchanged clinoptilolite.

The performed EDS analyses give numeric data (Tables 2 and 3) for barium content during the applied exchange procedures, which describe specific trends of exchange (Figure 3).

Table 2. Chemical composition (EDS, wt%) and structural formulae of Ba-clinoptilolite (90°) based on 72 oxygen atoms.

Samples Oxides	2 h	24 h	72 h	168 h	12 d	22 d
SiO <sub>2</sub>	66.24	60.39	60.49	60.81	59.22	59.50
Al <sub>2</sub> O <sub>3</sub>	11.43	10.58	10.85	10.99	10.82	10.88
MgO	0.22	0.19	0.16	0.03	–	–
CaO	2.29	1.13	0.73	0.72	0.44	0.20
Na <sub>2</sub> O	0.72	0.46	0.12	–	–	–
K <sub>2</sub> O	0.93	0.77	0.35	0.33	0.25	0.06
BaO	6.81	9.73	12.92	13.85	14.65	15.68
Σ	88.64	83.25	85.62	86.73	85.38	86.32
Atoms per formula unit (apfu)						
Si	29.91	29.84	29.71	29.68	29.62	29.62
Al	6.08	6.16	6.28	6.32	6.38	6.38
Mg	0.15	0.14	0.12	0.02	–	–
Ca	1.11	0.60	0.38	0.38	0.24	0.11
Na	0.63	0.44	0.11	–	–	–
K	0.54	0.485	0.22	0.20	0.16	0.04
Ba	1.20	1.88	2.49	2.65	2.87	3.06

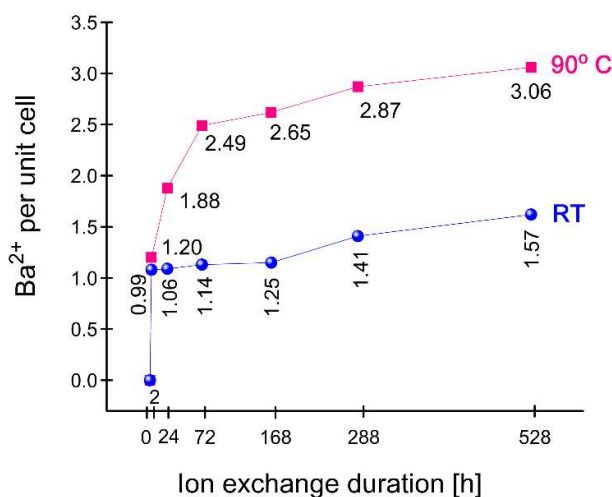


Figure 3. Exchanged Ba<sup>2+</sup> for different duration time and temperature (EDS data).

**Table 3.** Chemical composition (EDS, wt%) and structural formulae of Ba-clinoptilolite (RT) based on 72 oxygen atoms.

Samples Oxides	2 h	24 h	72 h	168 h	12 d	22 d
SiO <sub>2</sub>	68.93	55.06	69.12	60.71	68.26	62.72
Al <sub>2</sub> O <sub>3</sub>	12.31	9.77	12.21	10.77	12.19	11.09
MgO	0.30	0.23	0.29	0.22	0.24	0.21
CaO	2.74	2.08	2.48	2.15	2.35	2.13
Na <sub>2</sub> O	0.78	0.62	0.70	0.58	0.51	0.21
K <sub>2</sub> O	1.32	0.99	1.23	0.95	0.93	0.67
BaO	5.86	5.02	6.76	6.53	8.24	8.42
Σ	92.24	73.77	92.79	81.91	92.72	85.45
Atoms per formula unit (apfu)						
Si	29.74	29.77	29.79	29.77	29.74	29.79
Al	6.26	6.22	6.20	6.23	6.26	6.21
Mg	0.19	0.18	0.18	0.16	0.16	0.15
Ca	1.27	1.20	1.14	1.13	1.10	1.08
Na	0.65	0.65	0.58	0.55	0.43	0.19
K	0.72	0.68	0.67	0.59	0.52	0.41
Ba	0.99	1.06	1.14	1.25	1.41	1.57

These trends correspond to certain stages of ion exchange and practically last until the 22nd day (528 h) when 3 Ba<sup>2+</sup> cations per unit cell are exchanged at 90 °C (Figure 3). At RT the ion-exchange process is starting slowly and up to the 22nd day the maximum barium content is below 1.6 per unit cell, which is lower than the value (1.88) for the sample at 90 °C for 24 h. In the case of the high temperature Ba-exchange, the process is rapid and at 72 h the barium content is already high—2.49 per unit cell.

### 3.2. Rietveld Structural Analyses of Ba Exchange on Clinoptilolite with Time and Temperature

The starting Rietveld structural refinement was performed on the maximum Ba exchanged clinoptilolite—Ba-clinoptilolite (90 °C, 22 d) in order to fix the final Ba positions when all the original cations are exchanged.

The refinement of Ba-clinoptilolite finally converged at acceptable reliability factors (Table 4). Table 4 shows that the unit cell parameters of all studied Ba-exchanged samples are very similar except slight increase of the volume, *V*, from 2106.7 Å<sup>3</sup> (sample 90 °C, 2h) to 2107.9 Å<sup>3</sup> (sample 90 °C, 22 d).

**Table 4.** Reliability factors (R<sub>exp</sub>, R<sub>wp</sub>, R<sub>p</sub>, GOF, R<sub>B</sub>) and refined unit cell parameters of Ba-clinoptilolite from the ion exchange sequence at 90 °C.

Samples Parameters	2 h	24 h	72 h	168 h	12 d	22 d
R <sub>exp</sub>	2.06	2.10	2.10	2.10	2.17	2.10
R <sub>wp</sub>	5.51	5.47	5.16	5.33	5.13	5.32
R <sub>p</sub>	4.06	3.99	3.80	3.87	3.78	3.89
GOF	2.67	2.61	2.46	2.54	2.36	2.54
R <sub>B</sub>	2.03	2.15	1.66	1.77	1.79	1.83
<i>a</i> (Å)	17.6784(7)	17.6845(9)	17.6848(11)	17.6861(8)	17.6869(10)	17.6872(6)
<i>b</i> (Å)	17.9478(9)	17.9507(10)	17.9516(10)	17.9507(9)	17.9542(9)	17.9527(8)
<i>c</i> (Å)	7.4074(3)	7.4000(4)	7.3973(4)	7.4002(3)	7.3954(3)	7.3958(2)
β (°)	116.317(2)	116.221(3)	116.186(3)	116.227(3)	116.169(3)	116.158(2)
<i>V</i> (Å <sup>3</sup> )	2106.7(2)	2107.3(2)	2107.4(2)	2107.5(12)	2107.7(2)	2107.9(2)

The difference powder XRD plot of sample Ba-clinoptilolite (90 °C, 22 d) after the final refinement stage is shown on Figure 4.

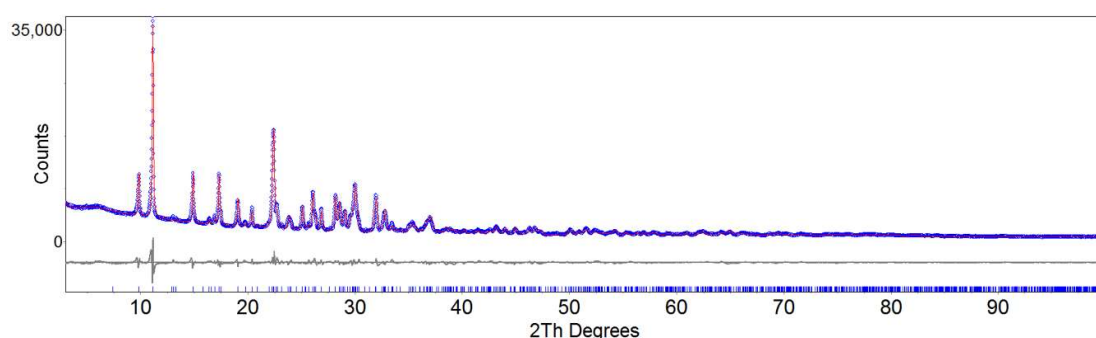


**Figure 4.** Difference plot of the powder XRD experimental and calculated pattern of Ba-clinoptilolite (90 °C, 22 d).

After the final stage of the refinements we obtained values for the structural parameters, which are reported in Table 5 for Ba-clinoptilolite (90 °C, 22 d) and Ba-clinoptilolite (90 °C, 2h) together with the interatomic distances reported in Table 6.

**Table 5.** Wyckoff positions (Wp), atomic coordinates, and occupancy factors of samples Ba-clinoptilolite (90 °C, 2h) and Ba-clinoptilolite (90 °C, 22 d).

Site	Atom	Wp	x	y	z	Occ 2 h	Occ 22 d
Si/Al	Si <sup>4+</sup>	8 j	0.1793(8)	0.1685(7)	0.0956(2)	1	1
Si/Al	Si <sup>4+</sup>	8 j	0.2885(8)	0.0898(7)	0.5002(2)	1	1
Si/Al	Si <sup>4+</sup>	8 j	0.2921(8)	0.3092(6)	0.2828(2)	1	1
Si/Al	Si <sup>4+</sup>	8 j	0.4356(9)	0.2012(7)	0.5887(2)	1	1
Si/Al	Si <sup>4+</sup>	4 h	0.0	0.2132(2)	0.0	1	1
O1	O <sup>2-</sup>	4 i	0.3047(2)	0.0	0.5494 (4)	1	1
O2	O <sup>2-</sup>	8 j	0.2684(2)	0.3798(9)	0.3889(3)	1	1
O3	O <sup>2-</sup>	8 j	0.3171(2)	0.3492(9)	0.1177(3)	1	1
O4	O <sup>2-</sup>	8 j	0.2385(2)	0.1047(2)	0.2545(3)	1	1
O5	O <sup>2-</sup>	4 g	0.5	0.1733(2)	0.5	1	1
O6	O <sup>2-</sup>	8 j	0.0821(2)	0.1586(2)	0.0636(3)	1	1
O7	O <sup>2-</sup>	8 j	0.3745(2)	0.2660(2)	0.4498(3)	1	1
O8	O <sup>2-</sup>	8 j	0.0086(2)	0.2677(9)	0.1850(2)	1	1
O9	O <sup>2-</sup>	8 j	0.2115(2)	0.2531(2)	0.1753(2)	1	1
O10	O <sup>2-</sup>	8 j	0.3839(2)	0.1275(9)	0.5997(2)	1	1
Na(M1)	Na <sup>+</sup>	4 i	0.1497(34)	0.0	0.6335(26)	0.157(34)	0
Ca(M2)	Ca <sup>2+</sup>	4 i	0.4584(30)	0.0	0.8014(65)	0.282(21)	0.031(12)
K(M3)	K <sup>+</sup>	4 i	0.2182(37)	0.5	1.0039(50)	0.136(13)	0
Mg(M4)	Mg <sup>2+</sup>	2 c	0	0	0.5	0.072(24)	0
Ba1	Ba <sup>2+</sup>	4 i	0.3550(25)	0.5	0.3237(66)	0.085(15)	0.131(10)
Ba2	Ba <sup>2+</sup>	4 i	0.2492(14)	0.5	0.0716(37)	0.156(48)	0.444(28)
Ba(Ca)	Ba <sup>2+</sup>	4 i	0.4818(59)	0	0.7820(42)	0	0.072(32)
Ba(K)	Ba <sup>2+</sup>	4 i	0.2275(37)	0.5	0.9952(31)	0.073(31)	0.114(29)
O11	O <sup>2-</sup>	4 j	0.601(16)	0.0889(47)	0.941(14)	0.145(20)	0.450(21)
O12	O <sup>2-</sup>	4 i	0.4099(52)	0.0	0.7478(26)	0.520(30)	0.243(27)
O13	O <sup>2-</sup>	8 j	0.5774(32)	0.0816(21)	0.9728(39)	0.68(2)	0.31(3)
O14	O <sup>2-</sup>	2 b	0	0.5	0	1	0.92(12)
O15 2 h	O <sup>2-</sup>	8 j	0.4753(38)	0.4111(36)	0.5290(34)		
O15 22 d	O <sup>2-</sup>	4 h	0.5	0.3989(26)	0.5	0.41(3)	0.556(34)
O16 2 h	O <sup>2-</sup>	4 i	0.4410(26)	0.5	0.1802(41)		
O16 22 d	O <sup>2-</sup>	4 i	0.4790(21)	0.0	0.4033(20)	0.44(2)	0.30(1)
O17	O <sup>2-</sup>	4 i	0.4016(43)	0.0	−0.0029(16)	0.320(50)	0.476(30)
O18 2 h	O <sup>2-</sup>	4 i	0.3808(41)	0.5	0.4710(38)		
O18 22 d	O <sup>2-</sup>	4 i	0.3858(39)	0.5	0.4710(38)	0.154(4)	0.448(59)
O19 22 d	O <sup>2-</sup>	4 i	0.4017(38)	0.5	0.2630(67)	0	0.142(43)

**Table 6.** Interatomic distances of the extra-framework cations and H<sub>2</sub>O molecules of samples Ba-clinoptilolite (90 °C, 2 h) and Ba-clinoptilolite (90 °C, 22 d) (nonindicated sample cells correspond to both samples).

Sample	Atom 1	Atom 2	d(Å)	Sample	Atom 1	Atom 2	d(Å)			
2 h 22 d	Ba1	Na	0.36(23)	2 h 22 d	K	O11 × 2	2.49(12)			
		O18	0.978(16)			O13 × 2	2.81(11)			
		Ba2	1.972(54)			O4 × 2	3.010(31)			
		O16	2.19(10)			O3 × 2	3.130(10)			
		O16	2.73(12)			Ca	O13 × 2	2.411(51)		
	2 h 22 d	Mg	2.301(12)		2 h 22 d	Ca	O13 × 2	2.506(62)		
			Ba(K)				2.481(12)	O1	2.524(27)	
			K1				2.530(23)	O14	2.642(45)	
			O15 × 2				2.553(32)	Ca	2.643(48)	
			O15 × 2				2.937(22)	O10 × 2	2.731(38)	
22 d		O2 × 2	2.808(14)	22 d		O11	O13	0.576(45)		
			O12				2.847(38)	O8	3.105(77)	
			O17				2.875(10)	O13	3.11(12)	
			O3 × 2				3.033(29)	O11	3.19(13)	
			Ba2				Ba(K)	0.52(12)	O12	O18
	22 d	K	0.55(19)		22 d	O12	O17	1.921(73)		
			Ba1				1.972(41)	O16	2.462(62)	
			Na				2.12(12)	O16	2.65(2)	
			O19				2.432(36)	O15 × 2	2.858(33)	
			O18				2.839(21)	O16	3.004(54)	
22 d		O11 × 2	2.849(23)	22 d		O13	O17	3.020(68)		
			O18				2.875(19)	O6 × 2	3.14(10)	
			O3 × 2				2.919(15)	O13	2.93(11)	
			O17				2.972(35)	O13	2.94(12)	
			O2 × 2				3.096(22)	O10	3.042(16)	
	2 h	O16	3.102(47)		2 h	O14	O8	3.068(22)		
			Ba(Ca)				Ca	0.491(22)	O5	3.110(34)
			O13 × 2				2.209(49)	O15	O15	1.13(10)
			O14				2.24(11)	O18	2.21(10)	
			O11 × 2				2.483(240)	O16	2.564(30)	
2 h		Ca	2.781(20)	2 h		O16	O12	2.857(22)		
			O10 × 2				2.826(42)	O16	2.861(49)	
			O1				2.827(16)	O18	3.002(31)	
			O13 × 2				2.868(47)	O7	3.062(23)	
			Ba(Ca)				3.000(49)	O15	O16 × 2	1.926(21)
	22 d	Ba(K)	K		0.201(21)	22 d	O15	O19 × 2	2.59(16)	
			O11 × 2		2.62(11)			O18 × 2	2.653(40)	
			Na		2.64(19)			O7	3.166(54)	
			O19		2.83(11)			O17	1.217(62)	
			O4		2.88(15)			O18	2.78(16)	
2 h		O13	2.97(14)	2 h	O16		O18	3.08(11)		
			O3				3.065(20)	O16	1.288(16)	
			O17				3.07(10)	O19	1.30(15)	
			O18				0.72(20)	O18	1.92(56)	
			Mg				2.38(13)	O19	2.431(18)	
	2 h	O16	2.521(16)		2 h	O17	O12	2.652(21)		
			O12				2.542(17)	O17	2.690(11)	
			O15				2.554(14)	O6	2.917(34)	
			O2				2.64(13)	O4	3.004(16)	
			K				2.66(28)	O19	1.96(17)	
2 h		O1	3.07(11)	2 h		O17	O2	2.811(16)		
			O15				1.693(32)	O2	2.868(17)	
			O18				2.02(10)	O19	1.681(27)	
			O16				2.125(44)	O3	3.051(13)	
			O12				2.914(44)			



## 4. Discussion

### 4.1. Powder XRD and EDS Data Interpretation of Ba Exchanged Clinoptilolite

The EDS data confirms that the barium exchange on the studied clinoptilolite proceeds up to the 22nd day with different speed. Powder XRD analyses show marked intensity changes especially for peaks 020 and 200.

These intensity changes may be interpreted according to Petrov et al. [12]. The authors refined the structure of almost fully Ba<sup>2+</sup> exchanged clinoptilolite using powder XRD data. They comment the profound intensity changes in the powder XRD pattern. Later, Petrov [23] performed detailed crystal chemical calculations for the intensity change of 020 peak, theoretically showing the change of the structural factor  $F^2_{020}$  value related to different compositions of the exchangeable cationic complex in clinoptilolite, modelling the content with Li<sup>+</sup>, Na<sup>+</sup>, Ca<sup>2+</sup>, K<sup>+</sup>, Ba<sup>2+</sup>, Cs<sup>+</sup>, and Tl<sup>+</sup> ions in the plane of symmetry of the structure.

### 4.2. Rietveld Structural Interpretation of Ba Exchange on Clinoptilolite with Time and Temperature

The studied samples were taken at different hours of the ongoing ion exchange. It was proved that the cationic positions change their occupancy with time—from a partially to more fully occupied ones. The structural analysis of their population at different stages of the ion exchange process with respect to the extra-framework cations shows how the leaving of the outgoing cations takes place.

From the presented structural models one can get an idea whether the cations leave more or less simultaneously, whether they remain in the structure until the final stages of ion exchange, and whether they leave it completely or small amounts of them remain for up to 22nd day. In addition, a more detailed idea of how barium positions are filled during ion exchange is obtained.

The changes in the occupancy of the cationic positions during the ion exchange process can contribute to the elucidation of the logistic and transport possibilities of barium and outgoing cations in the structure of clinoptilolite at both temperature conditions.

The designed initial model of the Ba-clinoptilolite structure was based on the data of Larsen et al. [16] for natural Ba-heulandite (monoclinic system, space group C2/m). Specific step was to model the barium populations—about 3 atoms per unit-cell according to EDS data (Figure 3) at positions Ba1 and Ba2 determined by the above authors.

After a number of refinement cycles of sample Ba-clinoptilolite (90 °C, 22 d) (Figure 5) we found that the occupancy of position Ba1 lowers from 0.359 to 0.131 in our case and vice versa the occupancy of position Ba2 increases from 0.190 to 0.444, which correlates with the data of Petrov et al. [12]. The coordinates of these two barium positions in our Ba-clinoptilolite stay very close to those of Ba-heulandite [16]. In a cluster in the C ring (K + Ba1, Ba2, Figure 5) we found a third position, Ba(K) (Table 5) with occupancy 0.114, closely situated near the original potassium M3 position of Koyama and Takeuchi [7]. This position is slightly overlapping with Ba2 (at 0.52 Å) (Table 6) and their simultaneous occupation is forbidden. Additionally, we found a fourth slightly occupied (0.073) barium position noted Ba(Ca), this time placed in the 8-member ring of channel B near M2 one, which is originally calcium position (Koyama and Takeuchi [7]). A number of 9 H<sub>2</sub>O sites were additionally refined in the channels of Ba-clinoptilolite with varying occupancies, with some of them coordinating the barium cations (Figure 5, Table 5).

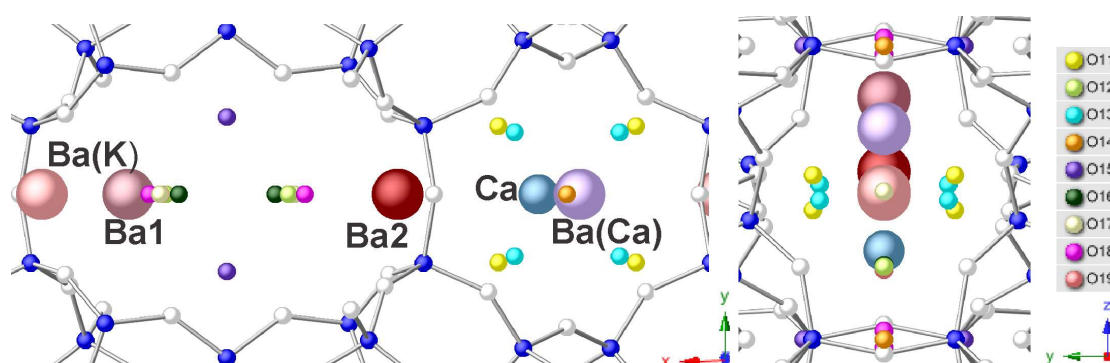


**Figure 5.** Structure representation of Ba-clinoptilolite (90 °C, 22 d). Left—channel A, middle—channel B, right—channel C.

The two dimensional channel system A and B parallel to (010) is crossed by channel C formed by eight-member rings. This is presented in Figure 5, where the cations (Ba in this case) appearing in different channels (A and B) but in channel C they are disposed in a continuous raw, observed in y-z projection.

According to Kirov et al. [17] there are two channels C and C', which cross channels A and B. In the present paper, we constructed a scheme for better representing the positioning cationic sites in the gallery structure of Ba-clinoptilolite (Figure 6).

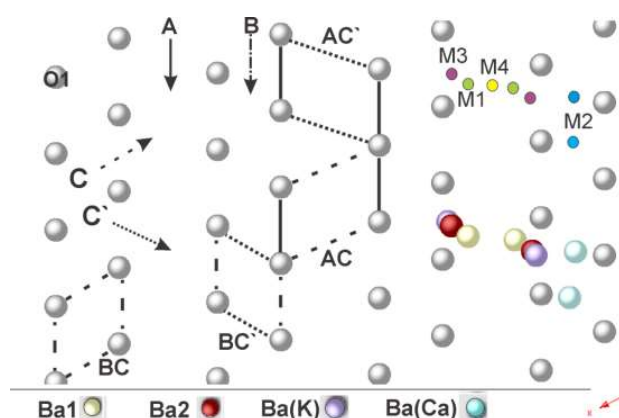


**Figure 6.** Gallery representation of the structure of Ba-clinoptilolite: distribution of O1 atoms in the plane 020, with directions of lanes A, B, C, and C' and location of the extra-framework cation positions and Ba positions.

The free space in HEU type structure [17] is formed as a unitary space by four lanes (or channels A and B parallel to [001], C to [100], and C' [100]) divided by pillaring aluminosilicate diortho-groups. Four framework oxygen atoms (O1) from the 72 ones (per unit cell) are bridge atoms between the neighbouring “layers-like” configuration, which explains the perfect (010) cleavage of the crystals. In the space between the “layers” the cation positions (lying on the *ac* symmetric plane) and the H<sub>2</sub>O molecules are situated, and this space can be described as a gallery space [17]. Kirov et al. [17] state that this gallery space can be decomposed into four systems of parallel cages, notated on Figure 6 AC, BC, AC', and BC'.

The above specified representation of the gallery-type structure for HEU group of minerals shows that each cation position belongs to gallery space and is located simultaneously in three lanes (channels). In such case, each cation position can be defined within two cages.

For cations in positions M1, M3, and M4 it is appropriate to be represented in cage AC' and position M2—in cage BC. From this perspective it cannot be proposed that the exchange of cations takes

place along the channels. In fact, the movement of H<sub>2</sub>O molecules and exchangeable cations through the “channel” system is not restricted by (Si, Al)O<sub>4</sub> barriers and in this sense, the entire channel space represents a different space configuration [17].

The negative charge of the framework comes mainly from the bridging oxygen atoms O1 of tetrahedron T2, keeping the extra-framework cations in the plane of symmetry and the preferred sites are occupied by particular cations depending on their charge and size. In clinoptilolite, the extra-framework cations occupy four positions (Figures 5 and 6). Positions M1 and M2 accommodate cations with a radius of around 1.0 Å (Na<sup>+</sup>, Ca<sup>2+</sup>). Position M3 is occupied by cations with larger ionic radii such as K<sup>+</sup> (1.31 Å) and Ba<sup>2+</sup> (1.35 Å). Position M4 is the only one which is not coordinated by framework oxygens and is occupied by Mg<sup>2+</sup>, surrounded only by H<sub>2</sub>O molecules. The cation positions are usually partially occupied.

In the case of Ba exchanged clinoptilolite for 22 days at 90 °C, barium ions prefer the position M3—described in this paper as split Ba2 and Ba(K), where 2.24 (per unit cell) cations dispose. The other portion of Ba<sup>2+</sup> is distributed as 0.52 cations in Ba1(M1) and 0.29 in Ba(Ca)·(M2), respectively.

A significant difference between clinoptilolite and heulandite is uncovered in the Al occupancy of the tetrahedral position T5, which is almost three times bigger in heulandites [17]. This is clearly illustrated by the ion exchange of the sample Ba-clinoptilolite (90 °C, 22 d), where the occupation of position Ba1 decreases sharply compared to that of natural barium heulandite from Norway [16].

The refined structure of Ba-clinoptilolite (90 °C, 22 d) is almost totally exchanged with barium cations (3.02 per unit cell) distributed in four cationic sites: Ba1, Ba2, Ba(K), and Ba(Ca) (Figures 5 and 6). Each site is with specific coordination including oxygen atoms from the tetrahedral framework and H<sub>2</sub>O molecules.

Position Ba1 is coordinated by four oxygen atoms (Figure 7) and four H<sub>2</sub>O molecules (O12, O15 × 2, O17) with interatomic bond distances from 2.81 Å to 3.03 Å. Position Ba2 is also coordinated by four oxygen atoms (Figure 7) and four H<sub>2</sub>O molecules (O11 × 2, O17, and O18) with interatomic bond distances from 2.85 Å to 3.10 Å. Position Ba(K) is coordinated by four oxygen atoms (O3 × 2, O4 × 2) (Figure 7) and four H<sub>2</sub>O molecules (O13 × 2, O17, O19) with interatomic bond distances from 2.83 Å to 3.07 Å. Position Ba(Ca) is coordinated by three oxygen atoms (O1, O10 × 2), (Figure 7) and two H<sub>2</sub>O molecules (O13 × 2) with interatomic bond distances from 2.83 Å to 2.87 Å. Positions Ba1, Ba2, and Ba(K) are similarly coordinated by four oxygen atoms from the framework and four H<sub>2</sub>O molecules. According to the performed Rietveld structure refinement position, Ba(Ca) appears less coordinated.

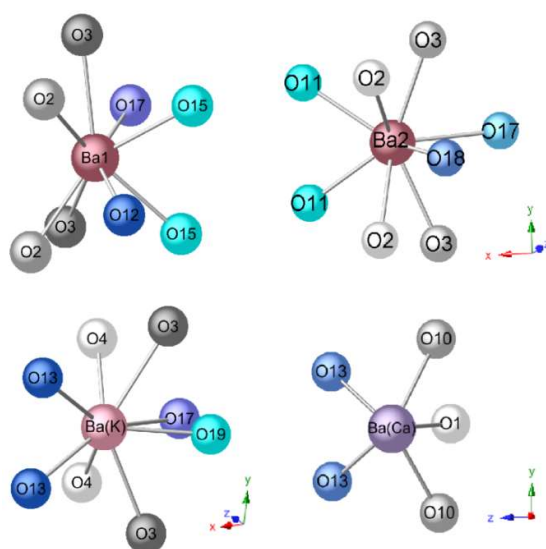


**Figure 7.** Coordination spheres of the barium positions in the structure of Ba-clinoptilolite (90 °C, 22 d)

#### 4.3. Movement of H<sub>2</sub>O Molecules and Ba<sup>2+</sup> Cations in the Clinoptilolite Structure During Barium Exchange

The coordinating oxygen and H<sub>2</sub>O positions around the sites of the outgoing cations in the structure of Ba-clinoptilolite (90 °C, 2 h) are given on Figure 8. The Na<sup>+</sup> position (M1-Na) according to Koyama and Takeuchi [7]) is coordinated by framework oxygens O2 × 2 and H<sub>2</sub>O molecules O12, O16, and O15 × 2. With the time of barium exchange, sodium ions leave the structure and H<sub>2</sub>O in position O15 is attracted to the coordination group of position Ba1 and O15 changed its atomic coordinates during the exchange process (Table 5, 2 h and 22 d). At the same time position O16 also changes its coordinates, lowers its occupancy, and finally does not coordinate position Ba1 in the case of sample Ba-clinoptilolite (90 °C, 22 d). Only position O12 preserves its coordinates around position Ba1. The H<sub>2</sub>O positions around the original position M3 (K) are preserved as coordinating Ba2 and Ba(K) in the almost completely exchanged sample Ba-clinoptilolite (90 °C, 22 d). For the original position M2 (Ca) the coordination is preserved for O1 and O13 but O14 with the time of ion exchange becomes forbidden for the occupation sphere of position Ba(Ca) in sample Ba-clinoptilolite (90 °C, 22 d) (Table 6, 2 h and 22 d).

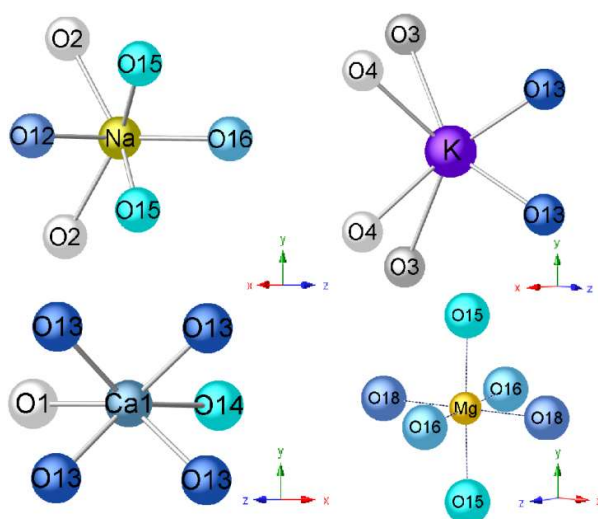


Figure 8. Outgoing cations coordination (2h of exchange).

On the basis of the above comments on the behaviour of the H<sub>2</sub>O molecules when coordinating the exchangeable cations, we may conclude that during the exchange process these molecules are attracted by incoming barium cations, thus making moves like H<sub>2</sub>O positions O15 and O18 but other like O16 lower their occupation, change their position, and finally do not participate in the coordination of the incoming cations (Ba<sup>2+</sup> in our case). In addition, the opposite case is observed. Position O17 is not a coordinating one in sample Ba-clinoptilolite (90 °C, 2 h) but later during the barium exchange it increases its occupancy and participates in the coordination of position Ba1. At the same time, a new H<sub>2</sub>O position (O19) appears in the coordination of position Ba(K).

All these changes in the positions of H<sub>2</sub>O molecules during the ion exchange process indicate intraspaces diffusion, together with exchangeable cations movements.

Rietveld refinements of the structures of the rest Ba-exchanged samples for 24 h, 72 h, 168 h, 12 d, and 22 d at 90 °C and RT, respectively were also performed. The important data at the final stage of refinements is the obtained number of atoms per cationic position (Tables 7 and 8), which well correlate with the data of EDS (Tables 2 and 3).

**Table 7.** Number of atoms per unit cell in the cationic positions of initial and Ba-exchanged clinoptilolite (Cpt) at 90 °C (after structural refinement).

Sample	M1 Ba1	M2 Ba (Ca)	~M3 (Ba2)	~M3 Ba(K)	M1 Na	M2 Ca	M3 K	M4 Mg	Total Ba <sup>2+</sup>
initial Cpt	–	–	–	–	1.0	1.84	0.92	0.38	–
2 h	0.34	–	0.63	0.29	0.63	1.12/	0.54	0.15/	1.26
24 h	0.35	–	1.22	0.37	0.44/	0.55/	0.47/	0.13/	1.94
72 h	0.37	0.23	1.48	0.40	0.16/	0.40/	0.22/	0.08/	2.48
168 h	0.38	0.27	1.51	0.42	–	0.38	0.18	0.03/	2.58
12 d	0.42	0.28	1.68	0.46	–	0.24	0.14	–	2.84
22 d	0.52	0.29	1.77	0.46	–	0.12	–	–	3.04

**Table 8.** Number of atoms per unit cell in the cationic positions of initial and Ba-exchanged clinoptilolite (Cpt) at RT (after structural refinement).

Sample	M1 Ba1	M2 Ba (Ca)	~M3 (Ba2)	~M3 Ba(K)	M1 Na	M2 Ca	M3 K	M4 Mg	Total Ba <sup>2+</sup>
initial Cpt	–	–	–	–	1.0	1.84	0.92	0.38	–
2 h	0.24	–	0.52	0.24	0.64	1.32	0.71	0.16	1
24 h	0.29	–	0.56	0.24	0.62	1.22	0.69	0.16	1.09
72h	0.33	–	0.60	0.25	0.56	1.16	0.68	0.15	1.18
168h	0.34	–	0.64	0.25	0.55	1.15	0.62	0.14	1.23
12d	0.36	0.08	0.81	0.26	0.44	1.04	0.56	0.13	1.48
22d	0.4	0.12	0.86	0.26	0.34	0.98	0.45	0.12	1.64

The barium cations during the ion exchange at 90 °C eagerly enter the clinoptilolite structure during the first 2 h reaching 1.26 barium per unit cell (Figure 9, left). In the same interval, a profound lowering of the number of all original cations is observed (Figure 9, right). Up to 72 h this exchange is still significant reaching about 2.50 cations and then continues more slowly up to the 22nd day. The tendency for the outgoing cations is the opposite—their contents lower accordingly. After 2 h all of them decrease rapidly their content and then leave the structure after different exchange times (Figure 9, right) except calcium, which preserves 0.12 cations per unit cell even after 22 days of exchange (Table 7).

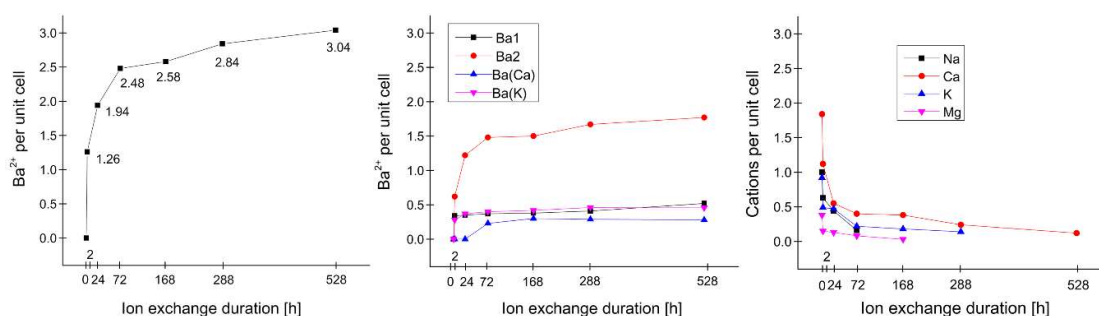
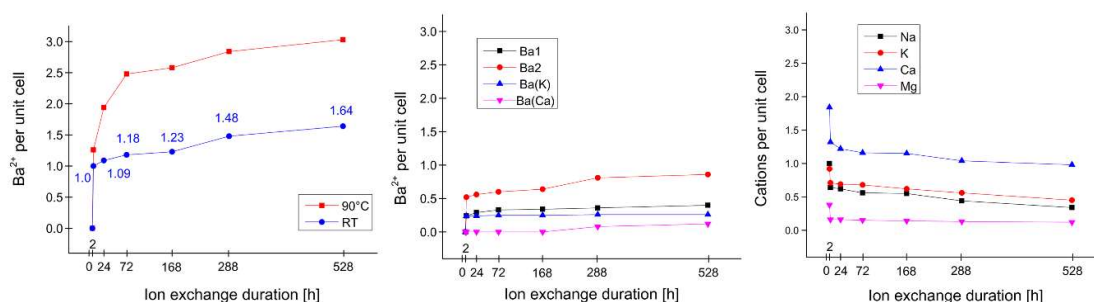
**Figure 9.** Extent of barium exchange (left), barium sites (middle) and outgoing cations (right) at 90 °C.

Figure 9 (middle) shows that the most populated position Ba2 (M3) is following the occupation trend of the total barium exchange (Figure 9, left). The other barium positions (Ba1, Ba(K), and Ba(Ca)) are occupied slightly at the first hours of the exchange process and with time there is only negligible increase of the occupancies. The calcium position Ba(Ca) (M2) starts to accept barium cations, noticed after 72 h of exchange and slightly changes its atomic coordinates (Table 5).

The barium exchange on clinoptilolite at room temperature (RT) (Figure 10, left) for the first 2 h proceeds similar to the exchange process at 90 °C (reaching 1.00 Ba<sup>2+</sup> per unit cell). However, in the following time intervals up to 72 h, the exchange proceeds very slowly and reaches 1.18 Ba<sup>2+</sup>, which is

more than twice as low as the sample at 90 °C. Then the barium exchange continues slowly (like the sample at 90 °C) reaching 1.64 Ba<sup>2+</sup> at the 22nd day.



**Figure 10.** Extent of barium exchange (left), barium sites (middle) and outgoing cations (right) at RT.

Concerning the occupancies of the barium positions during ion exchange at room temperature (RT) (Figure 10, middle, Table 8) again position Ba2 (around M3) is mostly exchanged with Ba<sup>2+</sup> but at 22 days is lower occupied (0.86 per unit cell) compared to the exchange at 90 °C. The trend of occupation of position Ba2 with time of exchange is similar to the total barium exchange at room temperature (Figure 10, left). The other positions are slowly occupied during the same time.

On Figure 10 (right) it is seen that the outgoing cations leave the structure quickly up to the first 2 h of the process and then their outgoing is slowed but at the 22nd day all of them are found to be present in small amounts (Table 8).

As a summary of the discussed above specificity of the barium exchange on clinoptilolite both at room temperature and 90 °C we may state that during the first 2 h we notice intensive barium exchange, predominantly realized in position Ba2. The outgoing cations (Na<sup>+</sup>, Ca<sup>2+</sup>, K<sup>+</sup>, and Mg<sup>2+</sup>) do not show any tendency of preferable leaving—they all together intensively leave the structure during the first 2 h and then this process is slowed down following the tendency of barium take up by clinoptilolite. This indicates that the exchangeable cations movement in the structure is realized easily without preferable directions, which shows that the diffusion process proceeds isotropically [16]. This conclusion fits well with the theory of gallery space in the HEU-type structure [17].

## 5. Conclusions

Clinoptilolite sample subjected to barium exchange for a period up to the 22 days at room temperature and 90 °C shows that the exchange process proceeds all the time with different speed. This is confirmed both by EDS analyses and Rietveld XRD structure refinement at different exchange times.

The starting Rietveld refinement was performed on the maximum Ba exchanged clinoptilolite (90 °C, 22 d). After refinement of unit-cell parameters, atomic occupancies and coordinates of exchangeable cationic sites and H<sub>2</sub>O molecules we determined four barium positions differently populated. A number of 9 H<sub>2</sub>O sites were additionally refined in the channels of Ba-clinoptilolite with varying occupancies, with some of them coordinating the barium cations.

The behaviour of the H<sub>2</sub>O molecules when coordinating the exchangeable cations during the exchange process shows that these molecules are attracted by incoming barium cations, thus making intraspace moves. Some of the H<sub>2</sub>O positions change their occupation and atomic coordinates. All these changes in the positions of H<sub>2</sub>O molecules during the ion exchange process indicate their diffusion accompanied by the exchangeable cations' movements.

The barium cations during the ion exchange at 90 °C eagerly enter the clinoptilolite structure during the first 2 h. In the same interval, a profound lowering of the number of all original cations is observed. Then the exchange process is gradually slower up (especially after 72 h) to the 22nd day. The tendency for the outgoing cations is the opposite—their contents lower accordingly. The barium exchange on clinoptilolite at room temperature for the first 2 h proceeds similar to the exchange process at 90 °C and then is slowed up to the 22nd day.

The performed barium exchange on clinoptilolite up to 22 days was chosen to study the process for a relatively long time. The expectation was to reach full exchange but at the end of the period the plateau is still not reached and 0.12 Ca<sup>2+</sup> still remain in the structure. With time, probably total exchange can be reached or the remaining calcium cations will be blocked for further exchange. The latter needs further investigation.

**Author Contributions:** Conceptualization, L.D.; methodology, L.D. and O.P.; software, L.D., Y.T., O.P., I.P., and F.U.; investigation, L.D., Y.T., O.P., I.P., and F.U.; writing—original draft preparation, L.D. and O.P.; writing—L.D., Y.T., and O.P.; visualization, L.D. and Y.T.; funding acquisition, L.D., Y.T., and O.P. All authors have read and agreed to the published version of the manuscript.

**Funding:** This work was financially supported by K2-2020 of IMC–BAS.

**Acknowledgments:** The authors of this paper are thankful to Project BG05M2OP001-1.002-0005 PERIMED, K2-2020 of IMC–BAS, and to the reviewers for their constructive comments and suggestions, which helped us to improve considerably the manuscript.

**Conflicts of Interest:** The authors declare no conflict of interest.

## References

1. Colella, C. Natural zeolites in environmentally friendly processes and applications. *Stud. Surf. Sci. Catal.* **1999**, *125*, 641–655.
2. Weitkamp, J. Zeolites and catalysis. *Solid State Ion.* **2000**, *131*, 175–188. [[CrossRef](#)]
3. Georgieva, I.; Benco, L.; Tunega, D.; Trendafilova, N.; Hafner, J.; Lischka, H. Multiple adsorption of NO on cobalt-exchanged chabazite, mordenite, and ferrierite zeolites: A periodic density functional theory study. *J. Chem. Phys.* **2009**, *131*, 054101. [[CrossRef](#)] [[PubMed](#)]
4. Shang, J.; Singh, G.; Li, R.; Gu, Q.F.; Nairn, K.M.; Bastow, T.J.; Medhekar, N.; Doherty, C.M.; Hill, A.J.; Liu, J.Z.; et al. Discriminative separation of gases by a “molecular trapdoor” mechanism in chabazite zeolites. *J. Am. Chem. Soc.* **2012**, *134*, 19246. [[CrossRef](#)] [[PubMed](#)]
5. Rodriguez-Iznaga, I.; Gomez, A.; Rodriguez-Fuentes, G.; Benitez-Aguilar, A.; Serrano-Ballan, J. Natural clinoptilolite as an exchanger of Ni<sup>2+</sup> and NH<sup>4+</sup> ions under hydrothermal conditions and high ammonia concentration. *Microporous Mesoporous Mater.* **2002**, *53*, 71–80.
6. Alberti, A. The crystal structure of two clinoptilolites. *Tschermaks. Min. Petr. Mitt.* **1975**, *22*, 25–37. [[CrossRef](#)]
7. Koyama, K.; Takeuchi, Y. Clinoptilolite: The distribution of potassium atoms and its role in thermal stability. *Z. Fur Krist.* **1977**, *145*, 216–239.
8. Petrov, O.E.; Karamaneva, T.A.; Kirov, G.N. Cation distribution in clinoptilolite structure: Natural samples. *Compt. Rend. Acad. Bulg. Sci.* **1984**, *37*, 785–788.
9. Yang, P.; Stolz, J.; Armbruster, T.; Gunter, M. Na, K, Rb, and Cs exchange in heulandite single crystals: Diffusion kinetics. *Am. Miner.* **1997**, *82*, 517–525. [[CrossRef](#)]
10. Yang, P.; Armbruster, T. Na, K, Rb, and Cs Exchange in Heulandite Single-Crystals: X-Ray Structure Refinements at 100 K. *J. Solid State Chem.* **1996**, *123*, 140–149. [[CrossRef](#)]
11. Hawkins, D.B.; Ordóñez, J.L. Preparation and properties of barium clinoptilolite. *Mater. Res. Bull.* **1972**, *7*, 543–550. [[CrossRef](#)]
12. Petrov, O.E.; Filizova, L.D.; Kirov, G.N. Cation distribution in clinoptilolite structure: Ba-exchanged sample. *Compt. Rend. Acad. Bulg. Sci.* **1985**, *38*, 603–606.
13. Cerri, G.; Sale, E.; Brundu, A. Solid-state transformation of (NH<sub>4</sub>, Ba)-clinoptilolite to monocelsian, mullite, and cristobalite. *Microporous Mesoporous Mater.* **2019**, *280*, 166–173. [[CrossRef](#)]
14. Nahr, T.H.; Bohrmann, G. Barium-rich authigenic clinoptilolite in sediments from the Japan Sea—A sink for dissolved barium? *Chem. Geol.* **1999**, *158*, 227–244. [[CrossRef](#)]
15. Dimova, L.; Shivachev, B.L.; Nikolova, R.P. Single crystal structure of pure and Zn ion exchanged clinoptilolite: Comparison of low temperature and room temperature structures and Cu vs. *Mo radiation Bulg. Chem. Commun.* **2011**, *43*, 217–224.
16. Larsen, A.O.; Nordrum, F.S.; Dobelin, N.; Armbruster, T.; Petersen, O.V.; Erambert, M. Heulandite-Ba, a new zeolite species from Norway. *Eur. J. Miner.* **2005**, *17*, 143–153. [[CrossRef](#)]

17. Kirov, G.; Dimova, L.; Stanimirova, T. Gallery character of porous space and local extra-framework configurations in the HEU-type structure. *Microporous Mesoporous Mater.* **2020**, *293*, 109792. [[CrossRef](#)]
18. Dimowa, L.T.; Petrov, O.E.; Djourellov, N.I.; Shivachev, B.L. Structural study of Zn-exchanged natural clinoptilolite using powder XRD and positron annihilation data. *Clay Miner.* **2015**, *50*, 41–54. [[CrossRef](#)]
19. Rietveld, H.M. Line profiles of neutron powder diffraction peaks for structure refinement. *Acta Crystallogr.* **1967**, *22*, 151–152. [[CrossRef](#)]
20. Rietveld, H.M. A profile refinement method for nuclear and magnetic structures. *J. Appl. Crystallogr.* **1969**, *2*, 65–71. [[CrossRef](#)]
21. *Topas V4.2: General Profile and Structure Analysis Software for Powder Diffraction*; Bruker AXS: Karlsruhe, Germany, 2009.
22. Krumm, S. WINFIT1.0—A computer program for X-ray diffraction line profile analysis. XIII Conference on Clay Mineralogy and Petrology. *Acta Univ. Carol. Geol.* **1994**, *38*, 253–261.
23. Petrov, O.E. Cation exchange in clinoptilolite: An X-ray powder diffraction analysis. In *Natural Zeolites '93 Occurrence, Properties, Use*; Ming, D.W., Mumpton, F.A., Eds.; ICNZ: Brockport, NY, USA, 1995; pp. 271–279.

**Publisher's Note:** MDPI stays neutral with regard to jurisdictional claims in published maps and institutional affiliations.



© 2020 by the authors. Licensee MDPI, Basel, Switzerland. This article is an open access article distributed under the terms and conditions of the Creative Commons Attribution (CC BY) license (<http://creativecommons.org/licenses/by/4.0/>).